Acetylshikonin (AceS) inhibited drug-resistant melanoma via downregulating matrix metalloproteinase-3 (MMP3)

Xin Zhao, Yu Zhang, Hui Cheng, Guiyuan Deng*

Xiangyang Hospital of Traditional Chinese Medicine (Xiangyang Institute of Traditional Chinese Medicine), China

Submitted: 28 May 2025; **Accepted:** 16 August 2025 **Online publication:** 17 October 2025

Arch Med Sci DOI: https://doi.org/10.5114/aoms/209585 Copyright © 2025 Termedia & Banach

Abstract

Introduction: Drug resistance has become a huge challenge in melanoma. This study aimed to explore the molecular mechanism by which acetylshikonin (AceS) inhibits melanoma with drug resistance to BRAF inhibitor (BRAFi). Material and methods: To identify potential targets of AceS in drug-resistant melanoma, we intersected AceS targets predicted by SwissTargetPrediction and differentially expressed genes in drug-resistant melanoma identified from the GSE203545 dataset. Drug-resistant M14 cells were treated with AceS with or without PLX4720, a BRAFi. Cell proliferation, migration, invasion, and apoptosis were investigated. MMP3 was quantified by qPCR and immunofluorescence. Extracellular matrix (ECM) was evaluated by MMP1 and MMP9. Also, drug-resistant M14 cells were transfected by MMP3 siRNA. Moreover, drug-resistant M14 cells with MMP3 overexpression were treated with AceS. *In vivo*, a subcutaneous tumor-bearing nude mouse model was established to validate the effects of AceS in drug-resistant melanoma.

Results: MMP3 was found to be the key target of AceS in drug-resistant melanoma. AceS significantly inhibited proliferation, migration, and invasion (p < 0.05), and promoted apoptosis (p < 0.05); it could increase the sensitivity of drug-resistant M14 cells to PLX4720 (p < 0.05). MMP3 silencing contributed to the decreases in proliferation, migration, and invasion, and the increased apoptosis (p < 0.05). Significantly, MMP3 overexpression reversed the effects caused by AceS (p < 0.05). AceS inhibited tumor growth; it reduced MMP1, MMP3, and MMP9 $in\ vivo$. AceS promoted tumor sensitivity to PLX4720 $in\ vivo$.

Conclusions: AceS downregulated MMP3 to modulate ECM remodeling, thereby inhibiting drug-resistant melanoma, and enhanced the cell response to BRAFi. Our findings provide intriguing insights into drug-resistant melanoma.

Key words: drug resistance, melanoma, acetylshikonin, matrix metalloproteinase-3.

Introduction

Melanoma, a highly aggressive malignancy arising from melanocytic transformation, predominantly manifests in cutaneous tissues and accounts for the majority of skin cancer-related mortality. Recent epidemiological data from the GLOBOCAN 2024 database reveal a concerning global incidence exceeding 330,000 newly diagnosed cases annually, un-

*Corresponding author:

Guiyuan Deng Xiangyang Hospital of Traditional Chinese Medicine (Xiangyang Institute of Traditional Chinese Medicine China

E-mail: dgyuansci@163.com

derscoring its significant public health burden [1]. Characterized by early metastatic dissemination and resistance to conventional therapies, melanoma progression is frequently driven by oncogenic mutations, among which B-raf proto-oncogene, serine/threonine kinase (BRAF) mutations serve as a principal molecular driver [2, 3]. Clinically, BRAF inhibitors (BRAFi) have transformed therapeutic paradigms, demonstrating substantial survival benefits in BRAF-mutant melanoma patients [4]. However, the long-term efficacy of BRAFi is invariably compromised by the emergence of acquired resistance [5]. Over 50% of patients develop therapeutic resistance within 12 months of BRAFi monotherapy, highlighting an urgent unmet clinical need [6]. It is crucial to find new methods or drugs to address the challenges of drug resistance in melanoma.

Matrix metalloproteinase-3 (MMP3) is a member of the matrix metalloproteinase (MMP) family, consisting of a translocation signal peptide, a propeptide, a catalytic domain, and a hemopexin domain [7]. Recently, MMP3 has been determined to affect many malignant tumors, including cervical cancer, triple-negative breast cancer, and ovarian cancer; it can orchestrate tumor progression by modulating critical biological processes such as angiogenesis, epithelial-mesenchymal transition (EMT), and metastatic dissemination [8-11]. In melanoma, MMP3 upregulation exhibits a robust correlation with enhanced migratory and invasive capacities of tumor cells, and pharmacological inhibition to MMP3 has been found to markedly attenuate these aggressive phenotypes, underscoring its pivotal regulatory role in melanoma pathogenesis [12]. Extracellular matrix (ECM) remodeling, a hallmark of tumor microenvironment (TME) plasticity, has been implicated in melanoma drug resistance development [13]. Mechanistically, ECM degradation disrupts biomechanical homeostasis within the TME, thereby promoting tumor cell survival and chemoresistance [14, 15]. Furthermore, MMP3 activation initiates a proteolytic cascade through upregulation of downstream effectors such as MMP1 and MMP9, collectively amplifying ECM remodeling to establish a permissive niche for metastatic invasion [7, 14, 16]. These findings strongly suggest that MMP3-mediated ECM dysregulation serves as a critical molecular bridge linking TME reprogramming to drug resistance in melanoma. MMP3 may thus represent a promising therapeutic target to reverse ECM-driven chemoresistance in melanoma treat-

Acetylshikonin (AceS), a bioactive naphthoquinone derived from the medicinal plant *Lithospermum erythrorhizon*, has recently emerged as a promising anti-cancer agent with multi-target

therapeutic potential [17, 18]. In a recent study, AceS demonstrated necroptosis-inducing capability in non-small cell lung cancer [19]. Its anti-tumor efficacy in osteosarcoma has been mechanistically linked to ROS-mediated metabolic reprogramming [20]. Particularly noteworthy are recent findings in melanoma research, where acetylshikonin exhibited significant suppression of metastatic behaviors through PI3K/Akt/mTOR pathway modulation [21]. However, the mechanism by which AceS inhibits melanoma progression has not yet been fully investigated.

Based on network pharmacology and molecular docking, this study investigated the potential targets of AceS and their biofunctions in BRAF-mutant melanoma and uncovered the biological relationship between AceS and MMP3 in the melanoma. We further determined that AceS was capable of exerting regulatory control over ECM remodeling processes by directly targeting MMP3, thereby suppressing the drug-resistant phenotype in BRAF-mutant melanoma. The findings of this study can provide novel insights into the dynamic regulatory network in the tumor microenvironment and targeted therapy in BRAF-mutant melanoma.

Material and methods

Screening of key targets of AceS in drugresistant melanoma

In this study, differentially expressed genes (DEGs) of BRAF-mutant melanoma with drug resistance were screened from the GSE203545 dataset using the DESeq 2 method, with $|\log_2(\text{foldchange})| > 1$ and FDR < 0.05. Potential targets of AceS were identified by SwissTargetPrediction (http://swisstargetprediction.ch/). Then, the intersection of AceS targets and melanoma DEGs was performed by Venn analysis. The correlation between intersection targets and survival of patients with melanoma were verified in the UALCAN database (https://ualcan.path.uab.edu/index.html).

Animals

BALB/c mice (6–8 weeks, 18–20 g) were housed at 21°C and 60% relative humidity. After 1-week habitation, mice were divided into: 1) the control group without administration of AceS and BRAFi; 2) the AceS group that received an intraperitoneal injection with AceS at the dose of 50 mg/kg; 3) the BRAFi group that received administration of PLX4720, a BRAFi, at the dose of 417 mg/kg, using tube feeding; 4) the AceS + BRAFi group receiving co-administration of AceS and PLX4720. All mice underwent subcutaneous injection of drug-resistant M14 cells (2 \times 10 $^{\circ}$ cells in the suspension). The administration was performed when

the volume of the subcutaneous tumor reached 100 mm³. This study was approved by the Animal Ethics Committee of the local hospital.

Dose of AceS in vitro

Drug-resistant M14 cells were treated with cell medium containing AceS at the concentrations of 0, 1, 2, 4, 8. 16, 32, 64, 128, 256, 512, 1024 $\mu mol/l$ for 24 h at 37°C. Cell viability was tested using a CCK-8 kit (C0037, Beyotime, Shanghai, China). Cell viability was calculated from the optical density (OD) measured on a microplate at 450 nm, as follows: cell viability (%) = (OD $_{\rm test\,concentration} - OD_{\rm blank})/$ (OD $_{\rm 0\,\mu mol/L} - OD_{\rm blank}) \times$ 100%.

Cells

Drug-resistant M14 cells (ATCC) were established by the gradient exposure protocol of PLX4720 [PMID: 24009868]. Then, drug-resistant M14 cells were divided into: the blank group without additional treatment, including BRAFi, AceS, and transfection; the excipient group with excipient treatment; the BRAFi group incubated with PLX4720-containing medium (1 μmol/l) for 24 h; the AceS group incubated with AceS-containing medium for 24 h; the AceS + BRAFi group incubated with the medium containing AceS and 1 µmol/l PLX4720 for 24 h; the AceS + oe-NC group receiving transfection of unloaded pcDNA3.1 plasmids and incubation with AceS-containing medium 48 h after transfection; the AceS + oe-MMP3 group receiving transfection of the MMP3 overexpression vector based on pcDNA3.1 and incubation with AceS-containing medium 48 h after transfection; the si-NC group receiving transfection of negative control of MMP3 siRNA; the MMP3 group receiving transfection of MMP3 siRNA.

Cell proliferation detected by CCK-8 assay

A total of 5×10^5 cells were added to 6-well plates and kept overnight at 37° C. 10μ l of CCK-8 reagent (C0037, Beyotime, Shanghai, China) was added. Cells were incubated for 1 h at 37° C. The OD value was read by a microplate (Thermo Fisher, USA) at 450 nm. Cell proliferation was calculated as follows: cell viability (%) = (ODtest-ODblank)/(ODcontrol-ODblank) × 100%.

Cell migration detected by wound healing

Cell migration was investigated by the wound healing assay. Briefly, cells (5×10^5 cells) were incubated in 6-well plates overnight at 37° C. A scratch on the cell monolayer by a clean tip was made at T = 0 h, and then cells were cultured for 24 h at 37° C. The images of the wounds were analyzed by ImageJ software to measure the width of

the wounds at T = 0 and 24 h. Cell migration was calculated using the following equation: cell migration (%) = $(width_{0h} - width_{24h})/width_{0h} \times 100\%$.

Cell invasion detected by Transwell inserts

The change in cell invasion was detected by Transwell inserts (diameter: 6.5 mm; pore size: 3.0 µm; 3472, Coring, 1 Riverfront Plaza, Corning, New York, USA). Before invasion assay, the upper chamber of Transwell inserts was pre-coated with 0.1 ml of 8% Matrigel (356234, Coring, 1 Riverfront Plaza, Corning, New York, USA) for 1 h at 37°C. Then, the upper chamber was supplemented with 100 μ l of cell suspension containing 1 \times 10⁵/ml, and the lower chamber contained 600 µl of serum-free DMEM, followed by incubation overnight at 4°C. The remaining cells in the upper chamber were removed, and 4% paraformaldehyde was used to fix cells for 30 min. Subsequently, the invasive cells were stained with 0.1% crystal violet for 30 min, followed by observation using a microscope (Olympus, Tokyo, Japan).

IF for MMP3

A total of 5×10^5 cells were plated into the 6-well plates and cultured overnight at 37°C. Cells were fixed with 4% paraformaldehyde for 30 min, and then washed with PBS 3 times. Cells were incubated with the blocking buffer containing 1% BSA for 30 min. Subsequently, cells were incubated with primary antibodies overnight at 4°C, including anti-MMP1 (ab137332, dilution: 1/50; Abcam, Massachusetts, USA), anti-MMP3 (ab52915, dilution: 1/100; Abcam, Massachusetts, USA), and anti-MMP9 (ab283575, dilution: 1/50; Abcam, Massachusetts, USA). Next, cells were incubated with the diluted secondary antibody (ab150077, dilution: 1/1000; Abcam, Massachusetts, USA) for 1 min, protected from light. Cells were mounted using Antifade Mounting Medium, and the images were captured with a fluorescence microscope.

IHC

Subcutaneous tumor sections were incubated with Antigen Retrieval Buffer for 5 min in a microwave oven after dewaxing and hydration. Then, the cooled down sections were incubated with 3% $\rm H_2O_2$ (88597, Millipore, Darmstadt, Germany) for 10 min at room temperature, and subsequently incubated with the blocking buffer containing 5% goat serum (C0265, Beyotime, Shanghai, China) for 30 min at room temperature. Sections were incubated with the diluted primary antibodies overnight at 4°C, followed by the HRP-conjugated secondary antibody (ab150077, dilution: 1/50; Abcam, Massachusetts, USA) for 1 h at room temperature. After DAB staining (P0202, Beyotime,

Shanghai, China), sections were stained with hematoxylin (C0107, Beyotime, Shanghai, China) for 2 min. Dehydration and clarification were performed, and then the neutral gum-mounted sections were observed by the microscope. The primary antibodies included anti-MMP1 (26585-1-AP, dilution: 1/100; Proteintech, Wuhan, China), anti-MMP3 (ab52915, dilution: 1/50; Abcam, Massachusetts, USA), anti-MMP9 (ab283575, dilution: 1/5000; Abcam, Massachusetts, USA) and anti-Ki-67 (ab16667, dilution: 1/200; Abcam, Massachusetts, USA).

Western blot

Cell lysates and tissue homogenate incubated with RIPA buffer were heated at 100°C for 10 min, and then centrifuged at 12,000 g for 10 min at 4°C. The quantification for protein concentration was performed using a BCA kit. The electrophoretic separation for proteins was performed by SDS-PAGE, followed by the trans-blotting onto PVDF membranes using a trans-blotting system (Bio-Rad, USA). The membranes were blocked by blocking buffer containing 5% skimmed milk for 1 h at room temperature. Next, the membranes were incubated with diluted primary antibodies overnight at 4°C, followed by incubation with HRP-conjugated goat anti rabbit antibody (ab6721, dilution: 1/10000; Abcam, Massachusetts, USA) for 1 h at room temperature. After being visualized by an ECL kit in the dark, blots were observed using a gel imaging system (Bio-Rad, USA). Primary antibodies included MMP1 (ab137332, dilution: 1/3000; Abcam, Massachusetts, USA), MMP9 (ab283575, dilution: 1/1000; Abcam, Massachusetts, USA) and GAPDH (ab9485, dilution: 1:2500; Abcam, Massachusetts, USA). GAPDH was used as a loading control.

qPCR

Total RNA extracted from cell or tissue samples was quantified by spectrophotometry (NanoDrop One/One, Thermo Fisher, USA), and then RNA samples with OD260/280>1.8 were used for qPCR. RNA was reverse transcribed to cDNA using a RevertAid RT Kit (K1691, Sangon, Shanghai, China),

Table I. Primer sequences

Primer	Sequence
GAPDH forward primer	5'-GTCTCCTCTGACTTCAACAGCG-3'
GAPDH reverse primer	5'-ACCACCCTGTTGCTGTAGCCAA-3'
MMP3 forward primer	5'-CACTCACAGACCTGACTCGGTT-3'
MMP3 reverse primer	5'-AAGCAGGATCACAGTTGGCTGG-3'

followed by quantification with Talent qPCR Pre-Mix (SYBR Green; FP209, TianGen, Beijing, China). Then, normalization was performed following the 2-AACt method. The primers of MMP3 and GAPDH are listed in Table I. GAPDH was used as a loading control.

Statistical analysis

All experiments were performed in triplicate. SPSS 25.0 software was used for the statistical analysis, and GraphPad 9.0 was used for the visualization of data. The comparison between two groups was performed using the independent t test, and the comparison between multiple groups (\geq 3 group) was performed using the one-way ANOVA test, followed by the post hoc Tukey test. P < 0.05 was considered statistically significant.

Results

AceS inhibited the proliferation, migration, and invasion of drug-resistant M14 cells and promoted their resensitization to BRAFi

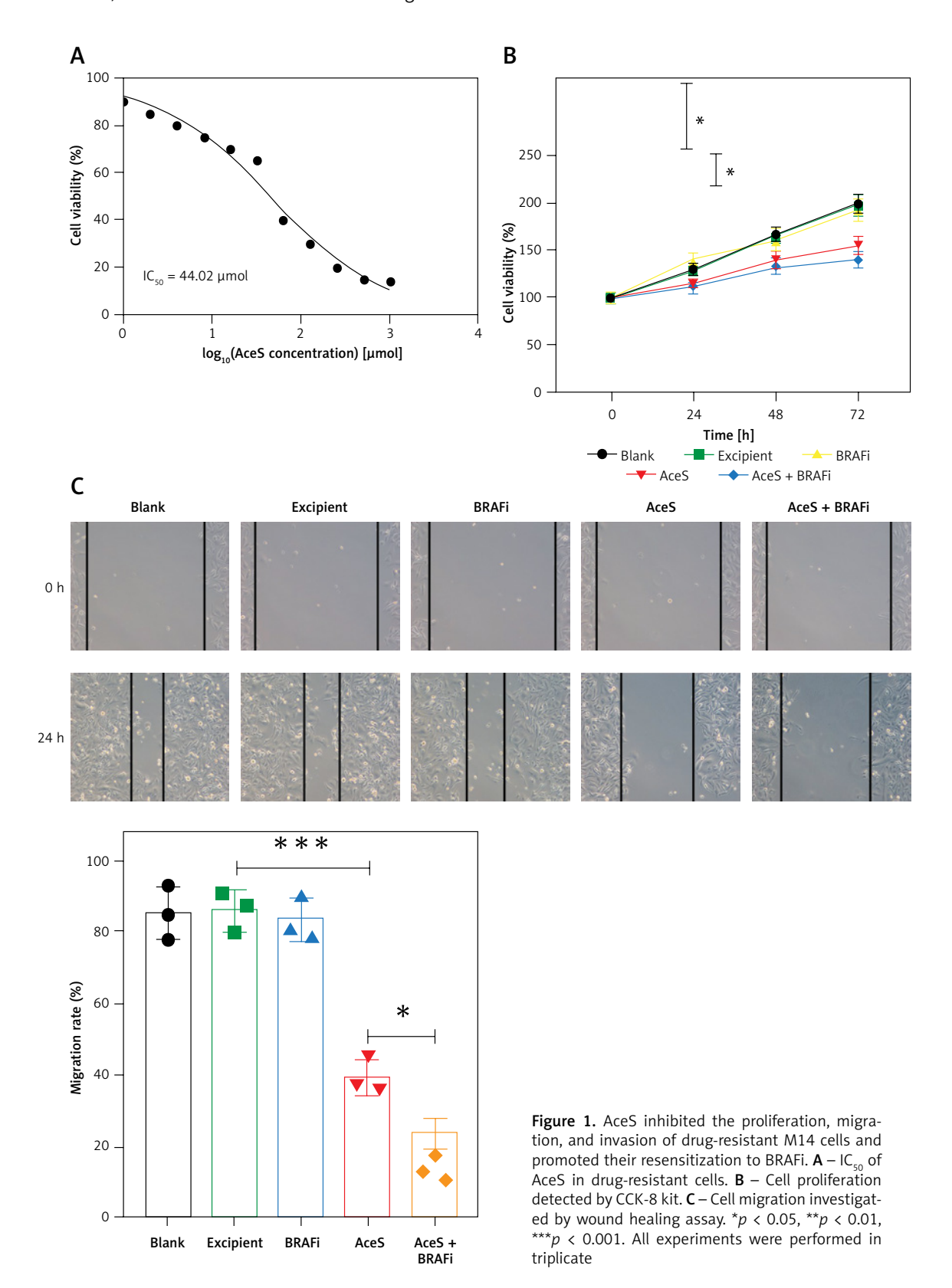
Drug-resistant M14 cells were treated with AceS at 1–1024 μ mol/l for 24 h, and then the IC₅₀ of AceS was calculated based on cell viability detected by CCK-8 assay. As shown in Figure 1 A, the IC_{50} of AceS was 44 μ mol/l. Then, cells were incubated with AceS-containing medium at 22 μ mol/l, 44 μmol/l, and 88 μmol/l. A significant decrease in cell viability was observed at 22 µmol/l, while no notable differences were detected at 44 and 88 µmol/l compared to the 22 µmol/l concentration. Thus, cells in the subsequent experiments were treated with 22 µmol/l AceS for 24 h. We found that the drug-resistant M14 cells showed higher cell proliferation, migration, and invasion and lower cell apoptosis as compared to M14 cells without drug resistance; BRAF inhibitor failed to reverse the changes in malignant behaviors of drug-resistant M14 cells (Figure 1). However, AceS treatment inhibited cell proliferation (Figure 1 B), migration (Figure 1 C), and invasion (Figure 1 D) in drug-resistant M14 cells and elevated the apoptotic M14 cells with drug resistance (Figure 1 E); intriguingly, AceS promoted drug-resistant M14 cells to respond to the BRAF inhibitor, including reductions in proliferation, migration, and invasion, and an increase in cell apoptosis (Figure 1).

MMP3 was a key target of AceS in drugresistant melanoma

We identified 99 targets of AceS using the SwissTargetPrediction database. Then, DEGs in drug-resistant M14 cells were screened from the dataset (GSE203545) recording the gene data of

BRAF-mutant melanoma with drug resistance. There were 363 genes differentially expressed in drug-resistant M14 cells, including 213 upregulated genes and 149 downregulated genes (Figure 2 A). Then, intersection of DEGs and AceS targets was

performed using Venn analysis. A total of 5 intersection targets were found: MMP1, MMP3, PTGS1, EGFR, and ABCG2 (Figure 2 B). We used the UALCAN database to analyze the correlation between overall survival of melanoma and 5 intersection



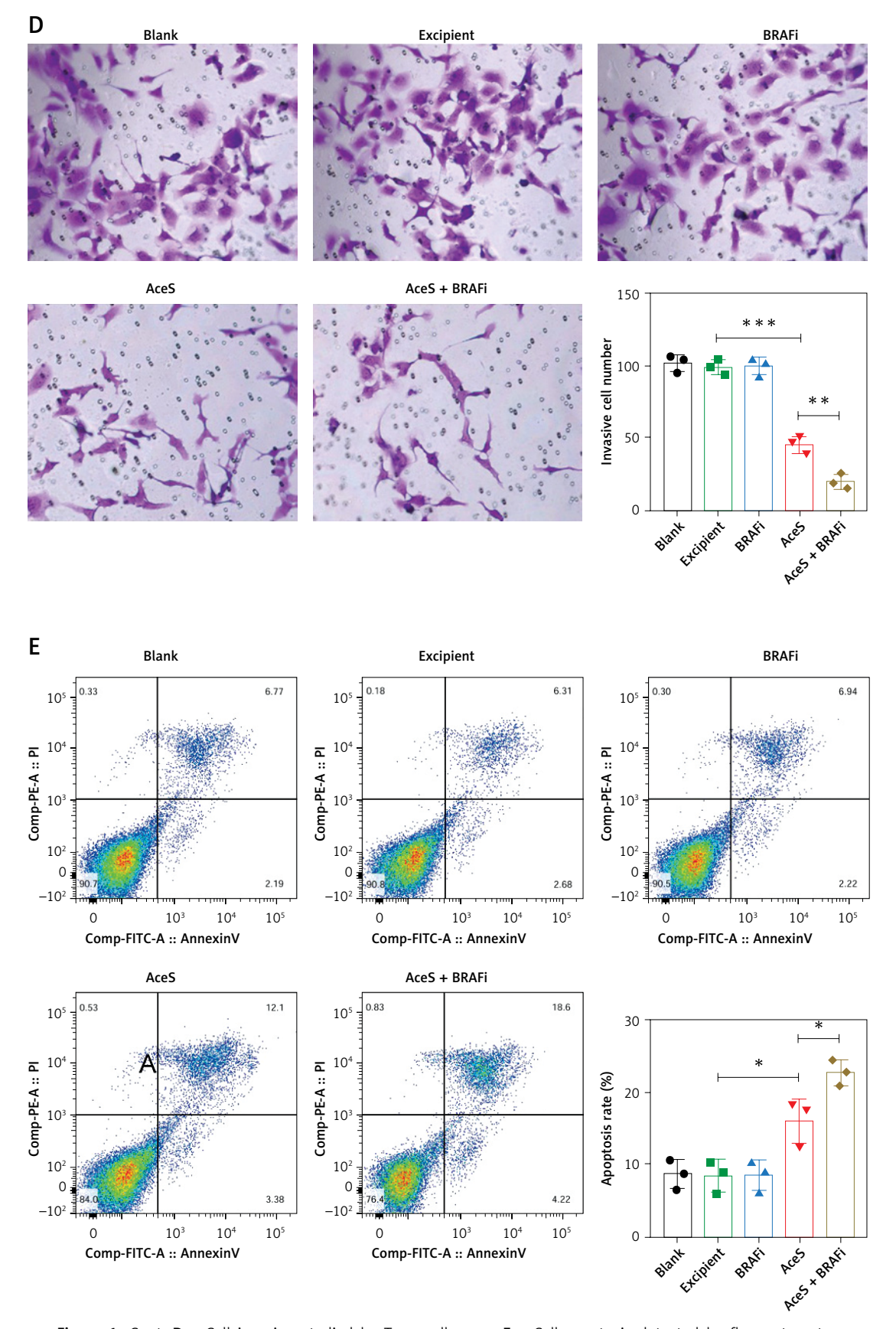
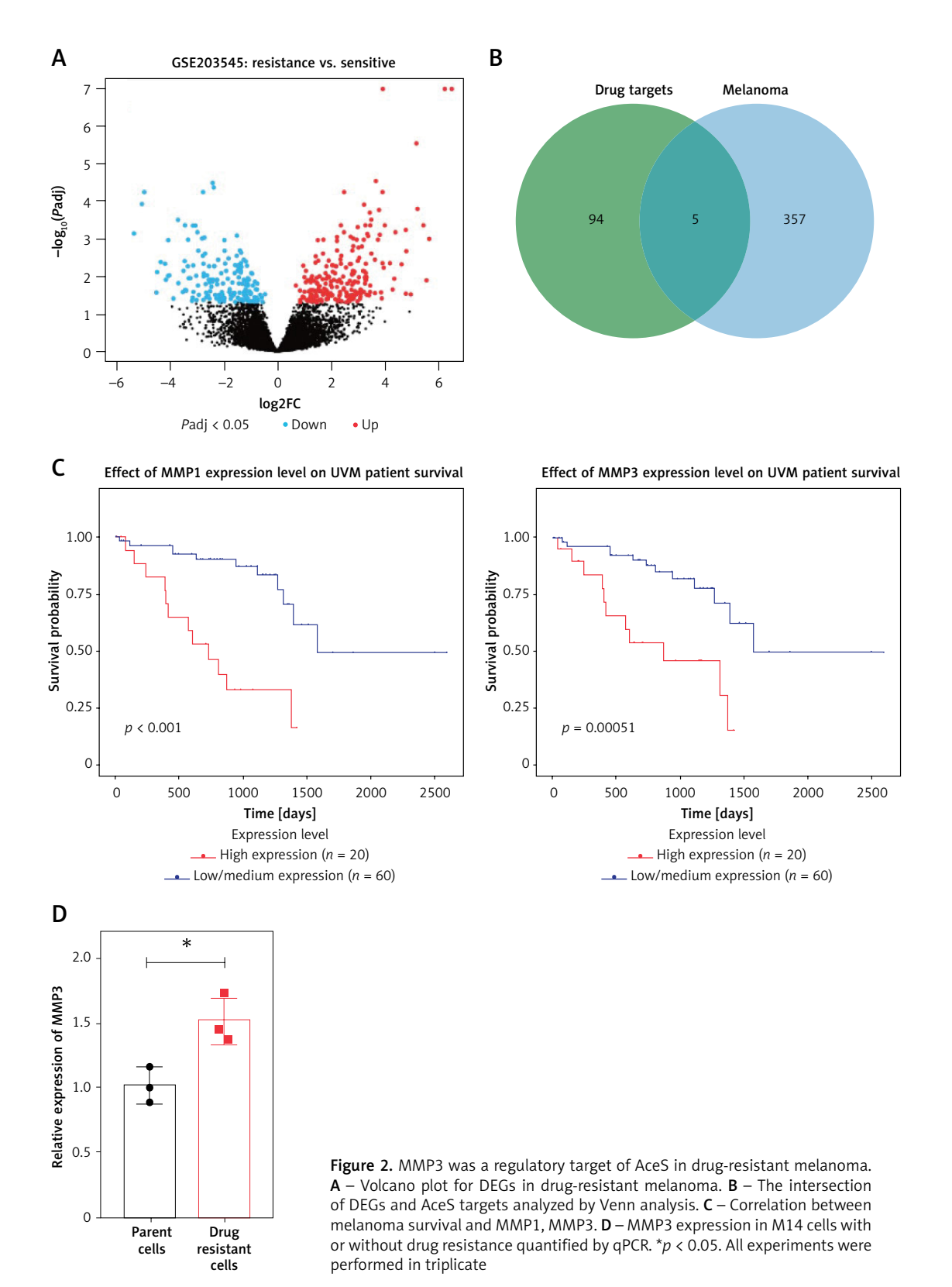


Figure 1. Cont. **D** – Cell invasion studied by Transwell assay. **E** – Cell apoptosis detected by flow cytometry. $^*p < 0.05, ^{**}p < 0.01, ^{***}p < 0.001$. All experiments were performed in triplicate

targets. As shown in Figure 2 C, the decreased overall survival was significantly correlated with higher expression of MMP1 and MMP3. According to the DEG analysis from GSE203545, MMP1 and MMP3 were increased in drug resistant mel-

anoma cells, and the expression of MMP3 (fold change: 3.324) was higher than that of MMP1 (fold change: 2.848). Therefore, we choose MMP3 as the core target of AceS. MMP3 in drug-resistant M14 cells was higher than that in parent cells (Fig-



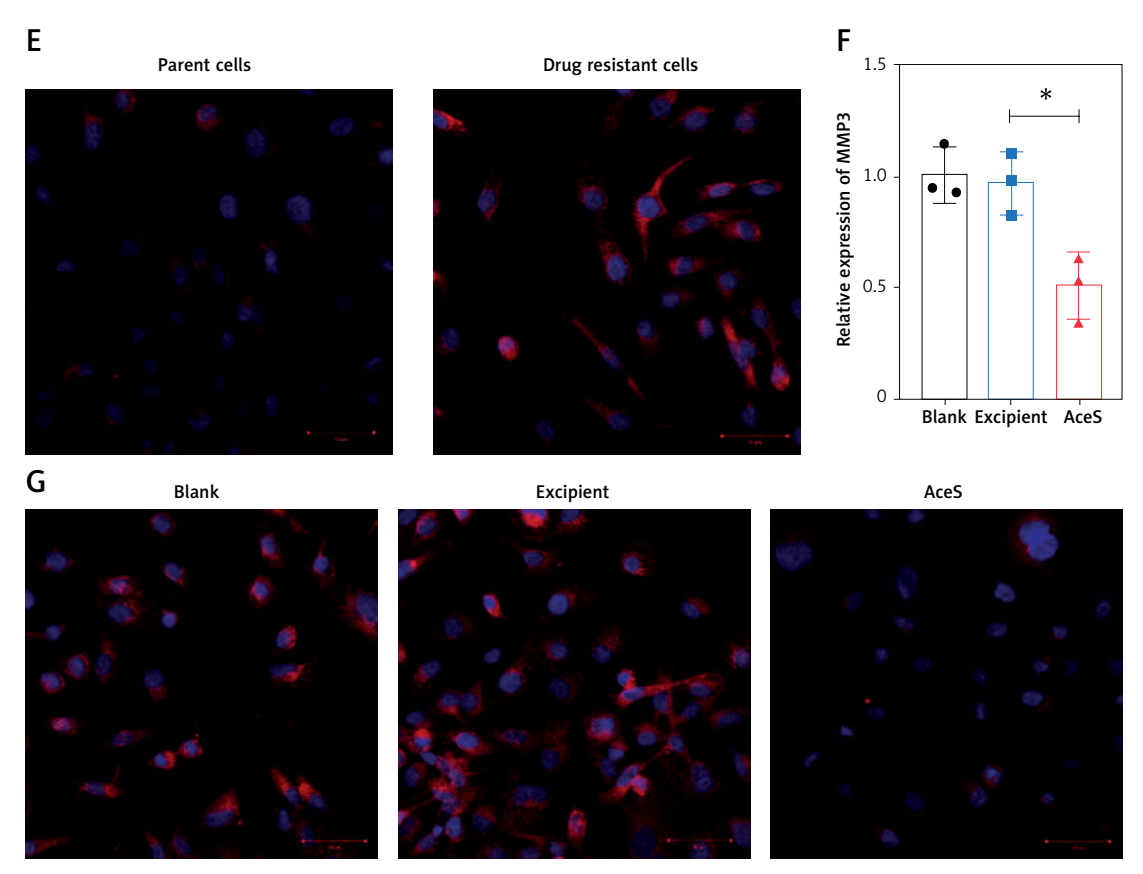


Figure 2. Cont. E-MMP3 in M14 cells with or without drug resistance measured by IF. F-MMP3 in blank, excipient, and AceS group detected by qPCR. G-MMP3 in blank, excipient and AceS group detected by IF. *p < 0.05. All experiments were performed in triplicate

ures 2 D, E). In drug-resistant cells, we found that MMP3 was downregulated because of AceS treatment (Figures 2 F, G), indicating that MMP3 might mediate the mechanism of AceS in BRAF-mutant melanoma with drug resistance.

Knockdown of MMP3 suppressed the growth and metastasis of drug-resistant M14 cells by modulating the extracellular matrix

Next, the role of MMP3 in regulating drug resistance in BRAF-mutant melanoma was studied. MMP3 in drug-resistant M14 cells was decreased by MMP3 specific siRNA (Figures 3 A, B). Downregulation of MMP3 contributed to the decreased proliferation (Figure 3 C) in drug-resistant M14 cells, and it inhibited the migration (Figure 3 D) and invasion of these cells (Figure 3 E); meanwhile, downregulation of MMP3 resulted in apoptosis in drug-resistant M14 cells (Figure 3 F). The development of drug resistance is involved in ECM remodeling. MMP3 is capable of regulating ECM remodeling, leading to decreased MMP1 and MMP9 expression in drug-resistant M14 cells; MMP3 silencing led to downregulation MMP1 and MMP9 (Figure 3 G).

AceS downregulated MMP3 to regulate the extracellular matrix, thereby inhibiting drug resistance and malignant behaviors in drug-resistant M14 cells

Overexpression of MMP3 was performed in drug-resistant M14 cells receiving AceS treatment (Figures 4 A, B). Significantly, MMP3 upregulation reversed the inhibitory role of AceS in drug-resistant M14 cells, observed as increases in proliferation (Figure 4 C), migration (Figure 4 D), and invasion (Figure 4 E), and a reduction in apoptosis (Figure 4 F). Moreover, MMP3 upregulation resulted in a decrease in MMP1 and MMP9 expression (Figure 4 G).

Validating the mechanism by which AceS downregulated MMP3 and suppressed drug resistance and tumor growth in mice with drug-resistant melanoma

An *in vivo* model of BRAF-mutant melanoma was used to investigate the therapeutic mechanism of AceS in the present study. AceS administration significantly reduced MMP3 expression in the subcutaneous tumor, whereas MMP3 did not respond to the BRAF inhibitor treatment (Figures 5 A, B). Then, we quantified the growth of

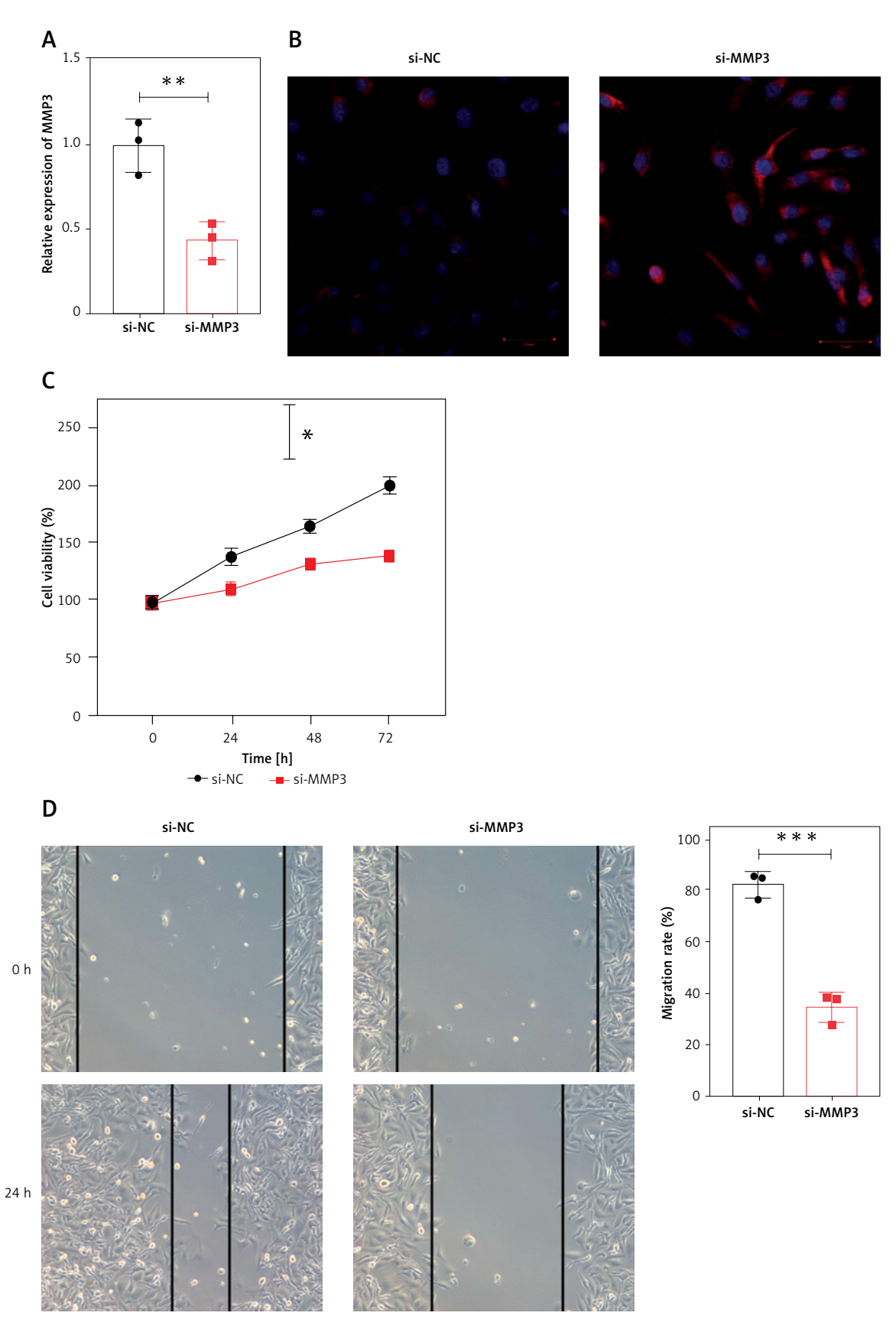


Figure 3. Knockdown of MMP3 suppressed the growth and metastasis of drug-resistant M14 cells by modulating the extracellular matrix. A - MMP3 expression in si-NC and si-MMP3 group detected by qPCR. B - MMP3 in si-NC and si-MMP3 group detected by IF. C - Cell proliferation detected by CCK-8 kit. D - Cell migration investigated by wound healing assay. *p < 0.05, **p < 0.01, ***p < 0.001. All experiments were performed in triplicate

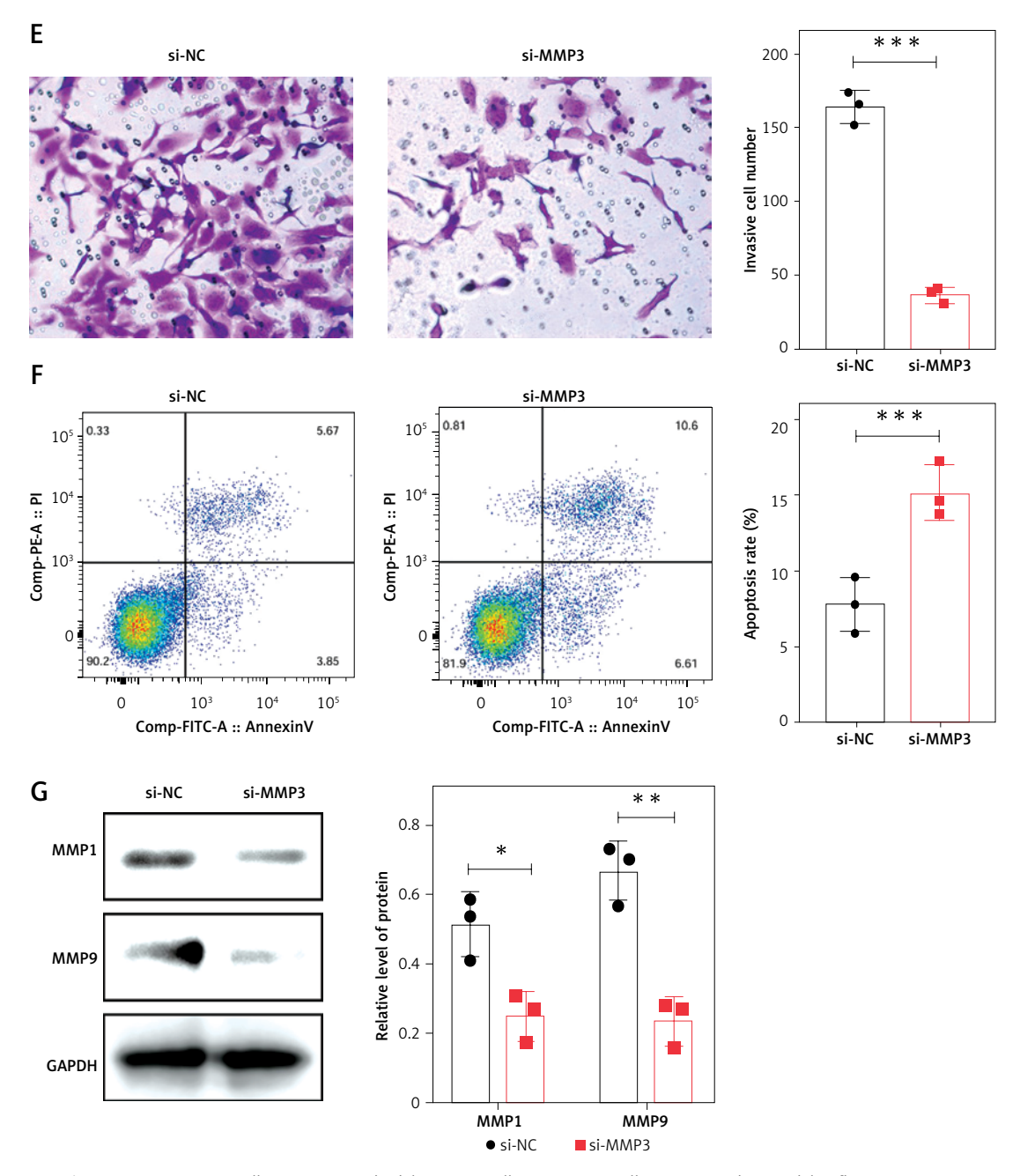


Figure 3. Cont. E – Cell invasion studied by Transwell assay. F – Cell apoptosis detected by flow cytometry. G – MMP1 and MMP9 in si-NC and si-MMP3 group. *p < 0.05, **p < 0.01, ***p < 0.001. All experiments were performed in triplicate

the subcutaneous tumor after treatment. BRAF inhibitor failed to inhibit the tumor growth in these nude mice; however, AceS administration led to a reduction in both volume and weight of the subcutaneous tumor (Figures 5 C, D). We also found that AceS led to downregulation of Ki-67, a marker of cancer cell proliferation, and it promoted Ki-67 downregulation in mice receiving BRAF inhibitor treatment (Figure 5 E). This indicated that AceS significantly inhibited cell proliferation in the subcutaneous tumor and promoted the drug sensitiv-

ity of the tumor to the BRAF inhibitor. Meanwhile, we measured MMP1 and MMP9 expression in the tumor. The AceS group showed reduced MMP1 and MMP9 expression as compared to the model group (Figure 5 F). There was no difference in expression of the two MMPs between the model and BRAF inhibitor groups (Figure 5 F). Nevertheless, the AceS + BRAF group showed lower expressions of MMP1 and MMP9 than these levels in the BRAF group (Figure 5 F).

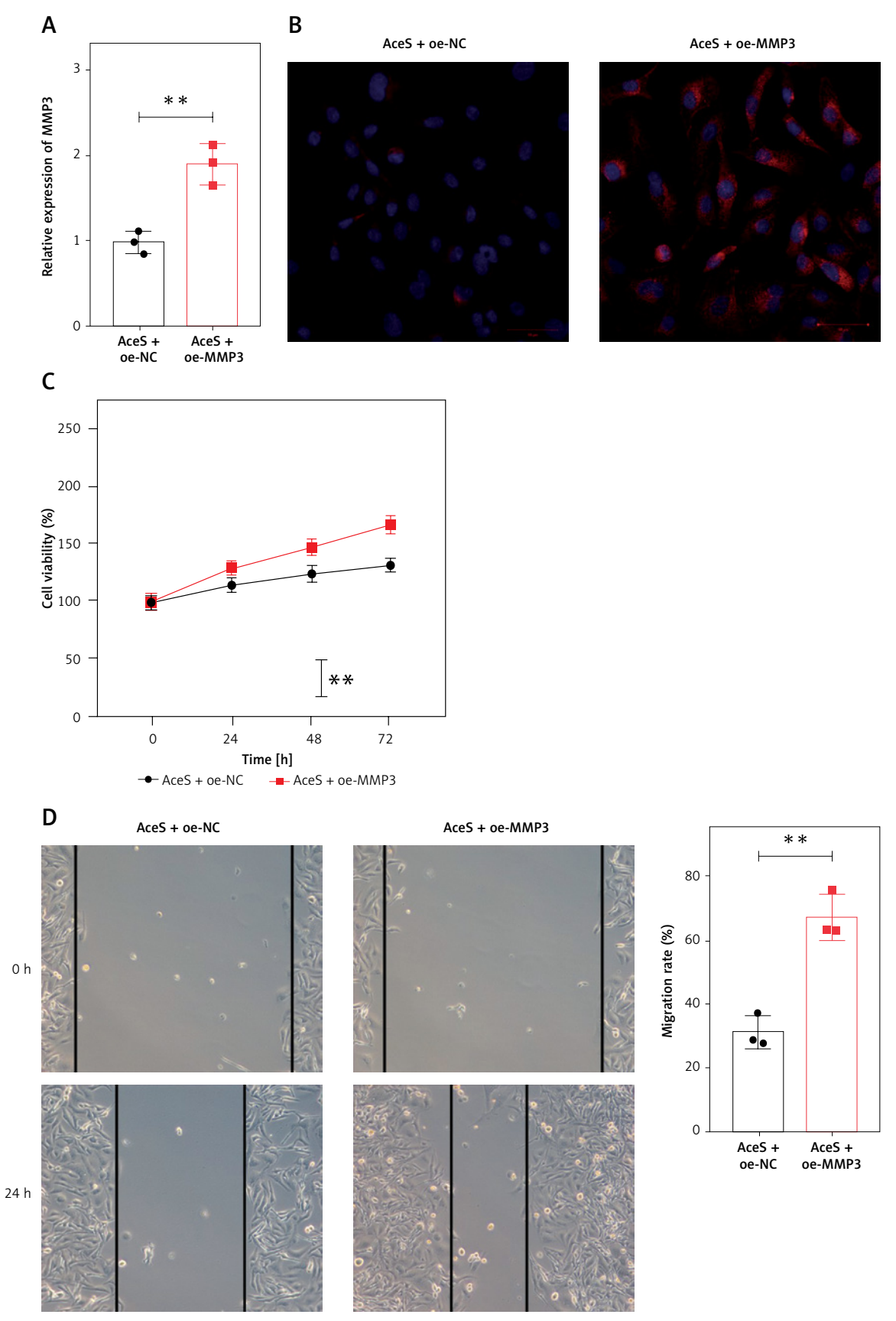


Figure 4. AceS downregulated MMP3 to regulate the extracellular matrix, thereby inhibiting drug resistance and malignant behaviors in drug-resistant M14 cells. **A** – MMP3 expression detected by qPCR. **B** – MMP3 detected by IF. **C** – Cell proliferation detected by CCK-8 kit. **D** – Cell migration investigated by wound healing assay. *p < 0.05, *p < 0.01, ***p < 0.001. All experiments were performed in triplicate

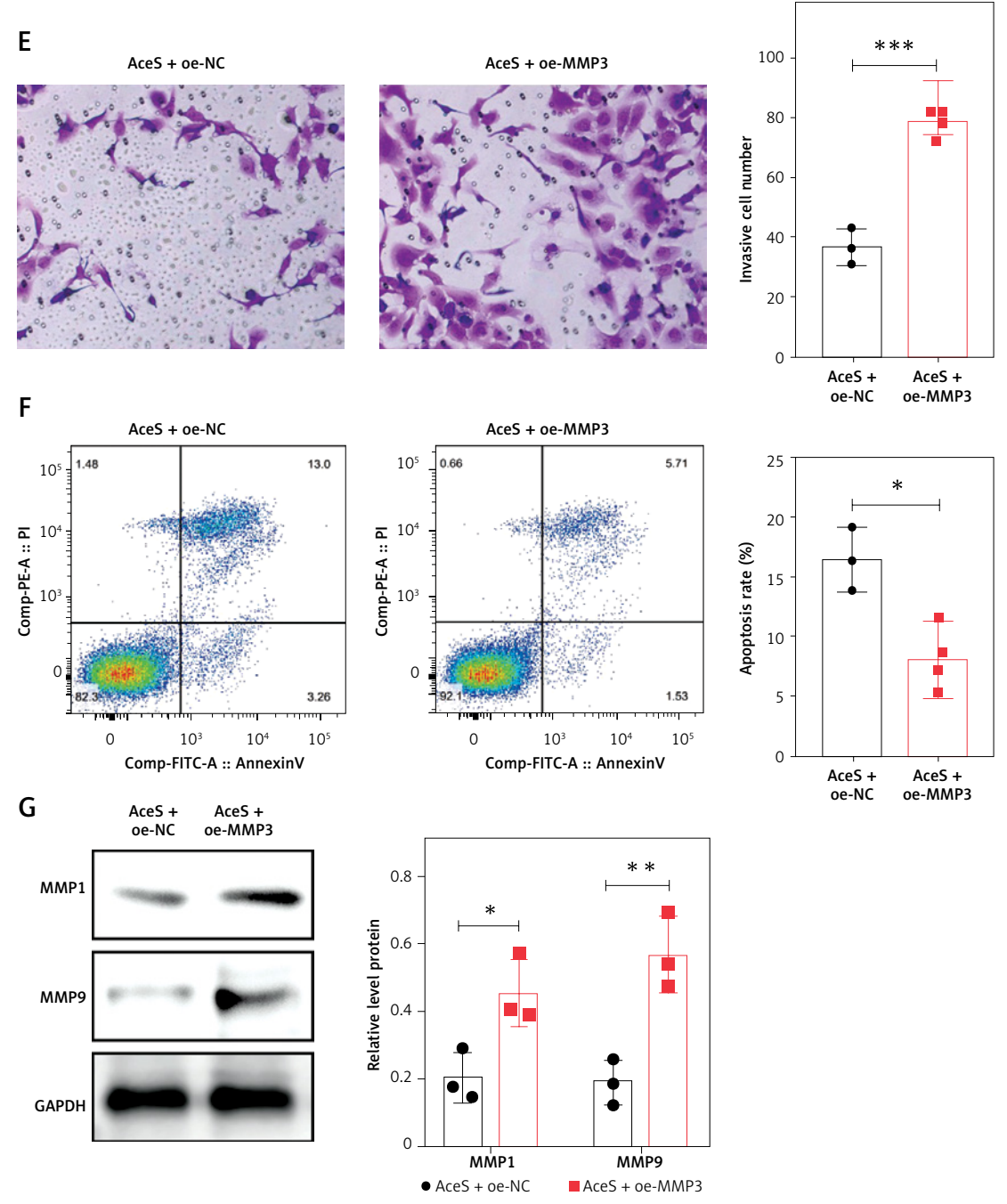


Figure 4. Cont. E – Cell invasion studied by Transwell assay. F – Cell apoptosis detected by flow cytometry. G – MMP1 and MMP9 detected by western blot. *p < 0.05, **p < 0.01, ***p < 0.001. All experiments were performed in triplicate

Discussion

Melanoma is correlated with activating mutations in the MAPK pathway such as BRAF. Although the therapeutic strategies of BRAF-mutant melanoma have evolved drastically over the decades, drug resistance still remains a huge challenge in the clinic. In fact, many patients with melanoma who benefited from BRAF inhibitor develop a tumor relapse within 1 year [22]. Thus, there is a lack of effective drugs to overcome the drug resistance in melanoma. In this study, we evaluated the an-

ti-tumor effect of AceS in BRAF-mutant melanoma, and found that AceS enhanced the response of BRAF-mutant melanoma to BRAFi treatment. Also, the molecular mechanism by which AceS inhibited drug resistance in BRAF-mutant melanoma via targeting MMP3-mediated ECM was explored.

AceS is a natural extract derived from *Lithospermum erythrorhizon*, a plant in the Boraginaceae family, and exhibits a broad range of pharmacological effects, including anti-inflammatory, lipid-regulating, and anticancer activities [23]. AceS can act as a non-selective cytochrome P450 inhib-

itor to modulate the drug metabolism [24]. Evidence indicated that AceS induced apoptosis and cell cycle arrest in chronic myeloid leukemia K562 cells by targeting the NF-κB pathway and inhibiting BCR-ABL [25]. Furthermore, AceS suppressed the progression of triple-negative breast cancer and HER2-positive breast cancer by reducing di-

hydrofolate reductase activity [26]. Our study established a BRAFi-resistant melanoma cell line and demonstrated that AceS treatment induced apoptosis while inhibiting proliferation, invasion, and migration, underscoring its potential for clinical application in BRAFi-resistant melanoma. Our findings also revealed that AceS enhanced cancer

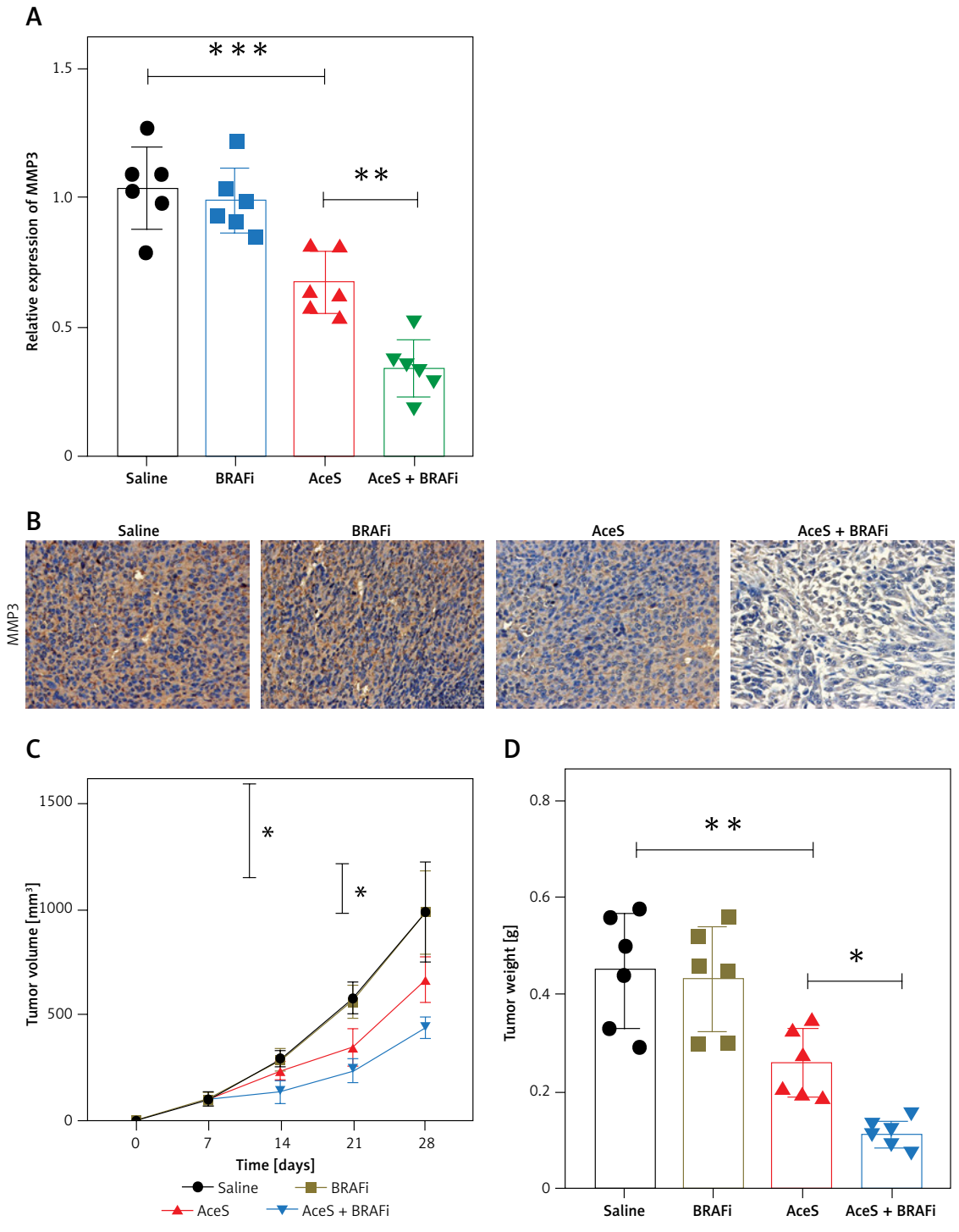


Figure 5. Validating the mechanism by which AceS downregulated MMP3 and suppressed drug resistance and tumor growth in mice with drug-resistant melanoma. A - MMP3 expression detected by qPCR. B - MMP3 measured by IHC. C, D - volume (C) and weight (D) of tumor. All experiments were performed in triplicate

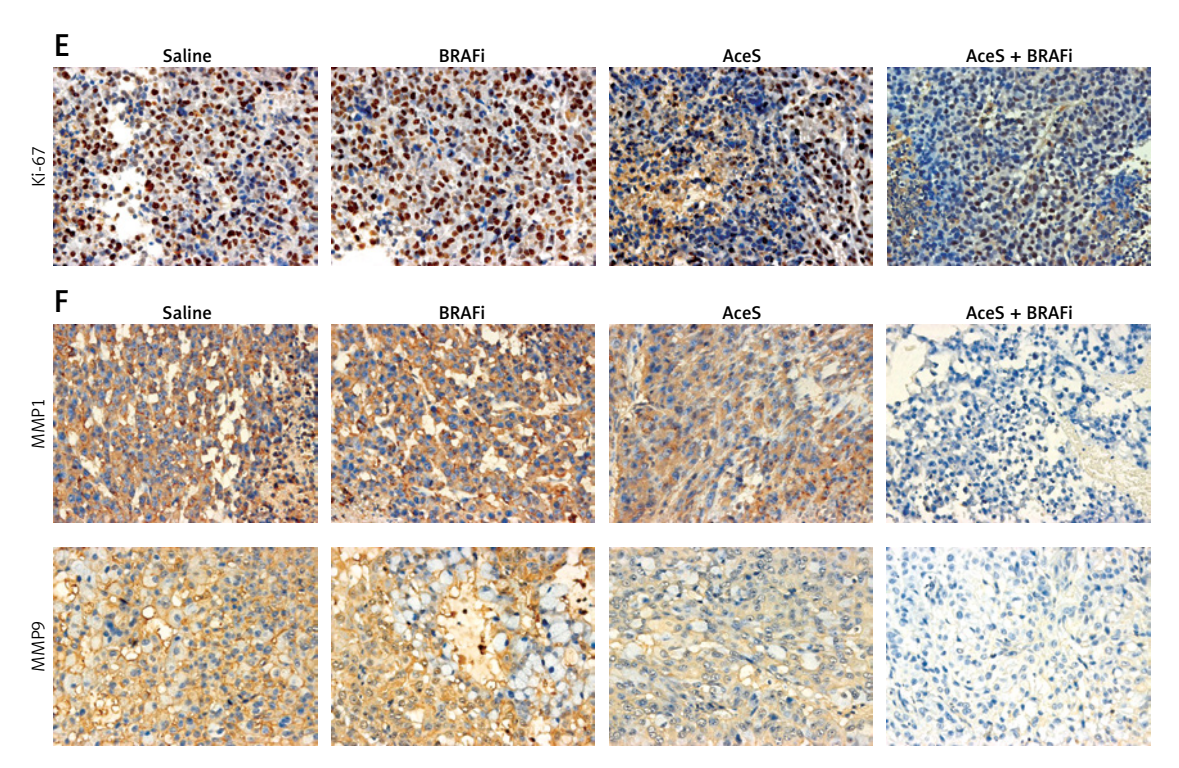


Figure 5. Cont. E – Ki-67 detected by IHC. F – MMP1 and MMP9 detected by IHC. All experiments were performed in triplicate

cell sensitivity to BRAFi, thereby reversing tumor drug resistance and amplifying anticancer efficacy. *In vivo* experiments further validated the dual antitumor and resistance-reversing effects of AceS.

Current scientific understanding of the anticancer mechanisms of AceS has remained incomplete. To address this, we adopted a network pharmacology approach to identify potential therapeutic targets of AceS in melanoma, including MMP1, MMP3, PTGS1, EGFR, and ABCG2. Analyses of the GSE203545 dataset and GEPIA database revealed that MMP3 was significantly upregulated in melanoma, with its overexpression strongly correlating with reduced overall survival in melanoma patients. MMP3, a matrix metalloproteinase, exhibits altered expression patterns linked to poor prognosis in primary prostate cancer [27], oral squamous cell carcinoma [28], and esophageal carcinoma [29]. Mechanistically, MMP3 suppressed tumor initiation and progression by inhibiting Erk1/2 and NF- B pathways, thereby blocking proliferation and migration [30]. In 3D culture models, MMP3-enriched extracellular vesicles robustly promoted solid tumor growth, whereas MMP3-knockout vesicles lacked this effect [31]. These abovementioned findings collectively indicate the critical role of MMP3 in malignant tumor development. Our study demonstrated that MMP3 knockdown significantly inhibits proliferation, migration, and invasion while inducing apoptosis in drug-resistant M14 cells, underscoring the essential role of MMP3 in melanoma drug resistance. Aligned with network pharmacology predictions, we observed that AceS markedly suppressed MMP3 expression, and its combination with BRAFi further amplified this suppression. To validate causality, MMP3-overexpressing plasmids were transfected to counteract the AceS-induced effects. Subsequent assays showed that MMP3 overexpression effectively reversed the antitumor activity of AceS in drug-resistant melanoma. Thus, we proposed that AceS inhibited BRAFi-resistant melanoma progression primarily through MMP3 downregulation.

The development of drug resistance in melanoma is closely associated with the ECM. The ECM contains non-cellular components that support tumor growth and motility. Additionally, cancer cell-derived ECM components can induce an immunosuppressive microenvironment, thereby enhancing immune evasion and promoting cancer cell survival [32, 33]. In melanoma, structural alterations in the ECM can elevate interstitial pressure, leading to vascular collapse and compromised blood supply, which exacerbates hypoxia and drives tumor progression [34]. Notably, MMP3 played a pivotal role in ECM dynamics. As a matrix metalloproteinase, MMP3 regulated the activation of ECM components. It promoted ECM degradation (e.g., laminin, elastin, fibronectin) by activating MMP1 and MMP9, thereby driving ECM remodeling [35–37]. Our study demonstrated that both MMP3 knockdown and AceS treatment downregulated MMP1 and MMP9 in drug-resistant melanoma cells, whereas MMP3 overexpression

reversed this regulatory effect. Melanoma cells exhibited heightened sensitivity to ECM remodeling. Consequently, altered expression of MMP3, a central mediator, promoted rapid cellular responses. This mechanistic cascade explained how AceS suppressed the drug-resistant phenotype: by downregulating MMP3, it inhibited MMP1/MMP9 expression, disrupted ECM architecture, and ultimately curtailed melanoma progression.

Collectively, we demonstrated that AceS down-regulated MMP3 to modulate ECM remodeling, thereby inhibiting drug-resistant melanoma progression, and enhanced the cell response to BRAFi. Our findings provide a novel therapeutic strategy in BRAF-mutant melanoma, and provide intriguing insights into the molecular mechanism of AceS in melanoma.

Our study has the following limitations. First, although we employed network pharmacology to identify potential targets and associated substrates of AceS in treating drug-resistant melanoma, the downstream signaling pathways mediating its anticancer effects remain to be fully elucidated. Thus, future studies should build upon the functional enrichment analysis to investigate specific signaling pathways involved and validate them through both in vivo and in vitro experiments. Second, while we demonstrated the AceS-induced enhancement of BRAFi that highlighted the therapeutic potential of their combination in BRAFi-resistant melanoma, the optimal administration protocols for this dual therapy remain unexplored. Therefore, systematic evaluation of dosing ratios and administration strategies for AceS-BRAFi combinations using preclinical models is warranted to establish novel and effective therapeutic regimens for melanoma. Moreover, our findings derived from the M14 cell line may not represent the behavior or responses of other melanoma cells. Therefore, in subsequent studies, we will select additional melanoma cell lines for investigation and examine the mechanism by which AceS inhibits melanoma drug resistance.

Funding

No external funding.

Ethical approval

Not applicable.

Conflict of interest

The authors declare no conflict of interest.

References

1. Bray F, Laversanne M, Sung H, et al. Global cancer statistics 2022: GLOBOCAN estimates of incidence and

- mortality worldwide for 36 cancers in 185 countries. CA Cancer J Clin 2024; 74: 229-63.
- Long GV, Swetter SM, Menzies AM, Gershenwald JE, Scolyer RA. Cutaneous melanoma. Lancet 2023; 402: 485-502
- 3. Timar J, Ladanyi A. Molecular pathology of skin melanoma: epidemiology, differential diagnostics, prognosis and therapy prediction. Int J Mol Sci 2022; 23: 5384.
- 4. Colombino M, Casula M, Paliogiannis P, et al. Heterogeneous pathogenesis of melanoma: BRAF mutations and beyond. Crit Rev Oncol Hematol 2024; 201: 104435.
- 5. Zhong J, Yan W, Wang C, et al. BRAF inhibitor resistance in melanoma: mechanisms and alternative therapeutic strategies. Curr Treat Options Oncol 2022; 23: 1503-21.
- Chen W, Park JI. Tumor cell resistance to the inhibition of BRAF and MEK1/2. Int J Mol Sci 2023; 24: 14837.
- 7. Suhaimi SA, Chan SC, Rosli R. Matrix metallopeptidase 3 polymorphisms: emerging genetic markers in human breast cancer metastasis. J Breast Cancer 2020; 23: 1-9.
- 8. Shao L, Liu W, Zhang C, et al. The role and function of secretory protein matrix metalloproteinase-3 (MMP3) in cervical cancer. Iran J Public Health 2024; 53: 855-66.
- Seehawer M, Li Z, Nishida J, et al. Loss of Kmt2c or Kmt2d drives brain metastasis via KDM6A-dependent upregulation of MMP3. Nat Cell Biol 2024; 26: 1165-75.
- 10. Quinones-Diaz BI, Reyes-Gonzalez JM, Sanchez-Guzman V, et al. MicroRNA-18a-5p suppresses tumor growth via targeting matrix metalloproteinase-3 in cisplatin-resistant ovarian cancer. Front Oncol 2020; 10: 602670.
- 11. Lawicki P, Malinowski P, Motyka J, et al. Plasma levels of metalloproteinase 3 (MMP-3) and metalloproteinase 7 (MMP-7) as new candidates for tumor biomarkers in diagnostic of breast cancer patients. J Clin Med 2023; 12: 2618.
- 12. Nunomura J, Nakano R, Naruke A, et al. Interleukin-1beta triggers matrix metalloprotease-3 expression through p65/RelA activation in melanoma cells. PLoS One 2022; 17: e0278220.
- Zhou S, Lu J, Liu S, et al. Role of the tumor microenvironment in malignant melanoma organoids during the development and metastasis of tumors. Front Cell Dev Biol 2023; 11: 1166916.
- 14. Kalli M, Poskus MD, Stylianopoulos T, Zervantonakis IK. Beyond matrix stiffness: targeting force-induced cancer drug resistance. Trends Cancer 2023; 9: 937-54.
- 15. Marusak C, Thakur V, Li Y, et al. Targeting extracellular matrix remodeling restores BRAF inhibitor sensitivity in BRAFi-resistant melanoma. Clin Cancer Res 2020; 26: 6039-50
- Pittayapruek P, Meephansan J, Prapapan O, Komine M, Ohtsuki M. Role of matrix metalloproteinases in photoaging and photocarcinogenesis. Int J Mol Sci 2016; 17: 868
- 17. Lin H, Ma X, Yang X, et al. Natural shikonin and acetyl-shikonin improve intestinal microbial and protein composition to alleviate colitis-associated colorectal cancer. Int Immunopharmacol 2022; 111: 109097.
- 18. Zhang Z, Shen C, Zhou F, Zhang Y. Shikonin potentiates therapeutic efficacy of oxaliplatin through reactive oxygen species-mediated intrinsic apoptosis and endoplasmic reticulum stress in oxaliplatin-resistant colorectal cancer cells. Drug Dev Res 2023; 84: 542-55.
- 19. Lin SS, Chang TM, Wei AI, et al. Acetylshikonin induces necroptosis via the RIPK1/RIPK3-dependent pathway in lung cancer. Aging 2023; 15: 14900-14.
- 20. Cha HS, Lee HK, Park SH, Nam MJ. Acetylshikonin induces apoptosis of human osteosarcoma U2OS cells by trig-

- gering ROS-dependent multiple signal pathways. Toxicol In Vitro 2023; 86: 105521.
- Jiang S, Wang H, Guo Y, Liu Z, Song W. Acetylshikonin inhibits the migration and invasion of A375 cells by reversing EMT process via the PI3K/Akt/mTOR pathway. Biotechnol Biotechnol Equipment 2019; 33: 699-706.
- 22. Rossi A, Roberto M, Panebianco M, et al. Drug resistance of BRAF-mutant melanoma: review of up-to-date mechanisms of action and promising targeted agents. Eur J Pharmacol 2019; 862: 172621.
- 23. Zhang Z, Bai J, Zeng Y, et al. Pharmacology, toxicity and pharmacokinetics of acetylshikonin: a review. Pharm Biol 2020; 58: 950-8.
- 24. Shon JC, Phuc NM, Kim WC, et al. Acetylshikonin is a novel non-selective cytochrome P450 inhibitor. Biopharm Drug Dispos 2017; 38: 553-6.
- 25. Hao G, Zhai J, Jiang H, et al. Acetylshikonin induces apoptosis of human leukemia cell line K562 by inducing S phase cell cycle arrest, modulating ROS accumulation, depleting Bcr-Abl and blocking NF-kappaB signaling. Biomed Pharmacother 2020; 122: 109677.
- 26. Wang J, Iannarelli R, Pucciarelli S, et al. Acetylshikonin isolated from Lithospermum erythrorhizon roots inhibits dihydrofolate reductase and hampers autochthonous mammary carcinogenesis in Delta16HER2 transgenic mice. Pharmacol Res 2020; 161: 105123.
- 27. Olczak M, Orzechowska MJ, Bednarek AK, Lipinski M. The transcriptomic profiles of ESR1 and MMP3 stratify the risk of biochemical recurrence in primary prostate cancer beyond clinical features. Int J Mol Sci 2023; 24: 8399.
- 28. Polz A, Morshed K, Drop B, Polz-Dacewicz M. Could MMP3 and MMP9 serve as biomarkers in EBV-related oropharyngeal cancer. Int J Mol Sci 2024; 25: 2561.
- 29. Hu HF, Xu WW, Zhang WX, et al. Identification of miR-515-3p and its targets, vimentin and MMP3, as a key regulatory mechanism in esophageal cancer metastasis: functional and clinical significance. Signal Transduct Target Ther 2020; 5: 271.
- 30. Liang M, Wang J, Wu C, et al. Targeting matrix metalloproteinase MMP3 greatly enhances oncolytic virus mediated tumor therapy. Transl Oncol 2021; 14: 101221.
- 31. Taha EA, Sogawa C, Okusha Y, et al. Knockout of MMP3 weakens solid tumor organoids and cancer extracellular vesicles. Cancers 2020; 12: 1260.
- 32. Yuan Z, Li Y, Zhang S, et al. Extracellular matrix remodeling in tumor progression and immune escape: from mechanisms to treatments. Mol Cancer 2023; 22: 48.
- Prakash J, Shaked Y. The interplay between extracellular matrix remodeling and cancer therapeutics. Cancer Discov 2024; 14: 1375-88.
- 34. Popovic A, Tartare-Deckert S. Role of extracellular matrix architecture and signaling in melanoma therapeutic resistance. Front Oncol 2022; 12: 924553.
- 35. Vempati P, Karagiannis ED, Popel AS. A biochemical model of matrix metalloproteinase 9 activation and inhibition. J Biol Chem 2007; 282: 37585-96.
- Steenport M, Khan KM, Du B, et al. Matrix metalloproteinase (MMP)-1 and MMP-3 induce macrophage MMP-9: evidence for the role of TNF-alpha and cyclooxygenase-2. J Immunol 2009; 183: 8119-27.
- Alge-Priglinger CS, Kreutzer T, Obholzer K, et al. Oxidative stress-mediated induction of MMP-1 and MMP-3 in human RPE cells. Invest Ophthalmol Vis Sci 2009; 50: 5495-503.